Whispering gallery mode carousel – a photonic mechanism for enhanced nanoparticle detection in biosensing

S. Arnold[1*], D. Keng[1], S. I. Shopova[1], S. Holler[2], W. Zurawsky[1], and F. Vollmer[3]

[1]*MicroParticle PhotoPhysics Lab, Polytechnic Institute of NYU, Brooklyn, New York 11201, USA*
[2]*Novawave Technologies, Redwood Shores, California 94065*
[3]*The Rowland Institute, Harvard University, Cambridge, Massachusetts 02142, USA*
[*]*Corresponding author: SArnold935@aol.com*

Abstract: Individual nanoparticles in aqueous solution are observed to be attracted to and orbit within the evanescent sensing ring of a Whispering Gallery Mode micro-sensor with only microwatts of driving power. This Carousel trap, caused by attractive optical gradient forces, interfacial interactions, and the circulating momentum flux, considerably enhances the rate of transport to the sensing region, thereby overcoming limitations posed by diffusion on such small area detectors. Resonance frequency fluctuations, caused by the radial Brownian motion of the nanoparticle, reveal the radial trapping potential and the nanoparticle size. Since the attractive forces draw particles to the highest evanescent intensity at the surface, binding steps are found to be uniform.

OCIS codes: (230.3990) Micro-optical devices; (040.1880) Detection; (020.7010) Laser trapping

References and links

1. A. Ashkin and J. M. Dziedzic, "Optical Trapping and Manipulation of Viruses and Bacteria," Science **235,** 1517-1520 (1987).
2. F. Vollmer and S. Arnold, "Whispering-gallery-mode biosensing: label-free detection down to single molecules," Nature Methods **5**, 591-596 (2008).
3. A. M. Armani, R. P. Kulkarni, S. E. Fraser, R. C. Flagan, and K. J. Vahala, "Label-free, single-molecule detection with optical microcavities," Science **317**, 783-787 (2007).
4. T. M. Squires, R. J. Messinger, and S. R. Manalis, "Making it stick: convection, reaction and diffusion in surface-based biosensors," Nature Biotechnol. **26**, 417-426 (2008).
5. J. C. Knight, G. Chung, F. Jacques, and T. A. Birks, "Phase-matched excitation of whispering-gallery-mode resonances by a fiber taper," Opt. Lett. **22**, 1129-1131(1997).
6. L. Yang, T. Carmon, B. Min, S. M. Spillane, and K. J. Vahala, "Erbium-doped and Raman microlasers on a silicon chip fabricated by the sol-gel process," Appl. Phys. Lett. **86**, 091114 (2005).
7. S. Arnold, M. Khoshsima, I. Teraoka, S. Holler, and F. Vollmer, "Shift of whispering-gallery modes in microspheres by protein adsorption," Opt. Lett. **28,** 272-274 (2003).
8. $L \approx (\lambda/4\pi)(n_s^2-n_m^2)^{-1/2}$, $D = 2n_m^2 (2n_s)^{1/2}(n_{np}^2 - n_m^2)/(n_s^2 - n_m^2)(n_{np}^2 + 2n_m^2)$, where n_s, n_m, and n_{np} are the refractive indices of the microsphere (1.45), aqueous medium (1.33), and nanoparticle (1.5 for virus and 1.59 for polystyrene; D = 1.50 and 2.26 respectively).
9. A. Ashkin, J. M. Dziedzic, J. E. Bjorkholm, and S. Chu, "Observation of a Single-Beam Gradient Force Optical Trap for Dielectric Particles," Opt. Lett. **11,** 288-290 (1986).
10. Y. Roichman, B. Sun, Y. Roichman, J. Amato-Grill, and D. G. Grier, "Optical forces arising from phase gradients," Phys. Rev. Lett. **100,** 013602 (2008).
11. J. N. Izraelachvili, *Intermolecular And Surfaces Forces.* 173-191 (Academic Press, Inc. , San Diego, CA, 1987).
12. I. Teraoka and S. Arnold, "Theory of resonance shifts in TE and TM whispering gallery modes by nonradial perturbations for sensing applications," J. Opt. Soc. Am. B **23,** 1381-1389 (2006).
13. F. Vollmer, S. Arnold, and D. Keng, "Single Virus Detection from the Reactive Shift of a Whispering-Gallery Mode," Proc. Natl. Acad. Sci. USA **105,** 20701-20704 (2008).
14. The translation from a size to a mass spectrum requires knowledge of mass density.

#107949 - $15.00 USD Received 25 Feb 2009; revised 31 Mar 2009; accepted 31 Mar 2009; published 1 Apr 2009

15. H. J. Yang, S. D. Moore, B. S. Schmidt, M. Klug, M. Lipson, and D. Erickson, "Optical manipulation of nanoparticles and biomolecules in sub-wavelength slot waveguides," Nature **457,** 71-75 (2009)

1. Introduction

Light forces interacting with mechanical systems provide a unique tool for studying small biological objects [1]. In the case of a whispering-gallery-mode (WGM) bio-sensor [2] where the intensity within the evanescent volume is built up resonantly a light-force may answer a puzzling question. Measured binding rates of bioparticles in aqueous solution using a toroidal WGM bio-sensor [3] at ultra-low concentrations appear to be about one hundred times higher than calculated based on diffusive and convective transport theory [4]. Traditionally Brownian motion of ultra-low concentration analytes crossing the boundary layer has been considered as a major hurdle for the practicality of miniature bio-sensors [4]. There is no comprehensive model to explain the physical mechanism of enhanced binding rates in the case of WGM bio-sensors. Here we report an observation and analysis of an optical mechanism that enhances the transport rate to the sensing volume of a microspherical silica resonator by more than 50x. Polystyrene nanoparticles are drawn toward this volume by evanescent optical gradient forces generated with just a few microwatts driving the resonator. At low ionic strength an addition electrostatic force repels the nanoparticle from the surface, contributing to a radial trap. Here the particle finds itself in the tangential momentum flux of the WGM and is driven to orbit by scattering forces. The radial trapping potential is elucidated from fluctuations in the micro-cavity's resonance frequency, allowing the use of the Carousel as a surface-potential nanoprobe. The maximum fluctuation enables the size and mass of the trapped nanoparticle to be determined without binding, suggesting that the WGM Carousel mechanism can be used for size/mass spectrometry in solution. At a considerably high ionic strength the electrostatic field is screened to a much shorter depth, and the particle is drawn closer to the surface where it is caught by a van der Waal interaction and binds. Resonance shifts due to these binding events are found to be steps having uniform heights.

2. The Whispering Gallery Mode Carousel Phenomenon

Nanoparticles suspended in an aqueous environment normally appear to be in Brownian motion. However, we observe in the vicinity of a bare silica microsphere (oblate microspheroid, eccentricity < 5%, equatorial radius $R \approx 50$ μm) excited into a circulating WGM (quality factor $Q \sim 10^6$), nanoparticles as small as 140 nm radius (a) are trapped for hundreds of seconds in orbit within the sensing volume with driving light power $P \approx 50$ μW. As shown in Fig. 1(a), these nanoparticles appear to circumnavigate in the direction that light takes within the WGM. The nanoparticle concentration was ≈ 1 fM in D_2O. D_2O (Aldrich, 99.9%) was used to minimize absorption loss in the infrared. The particle recorded in the video was seen to orbit for over two revolutions before escaping, Fig. 2.

A tapered fiber which coupled power into the microsphere was positioned a few microns to one side of the equator. At resonance, a dip was observed in the power transmitted through the fiber at wavelength λ_r as the laser was tuned. The power P driving the WGM was estimated from this dip depth [5, 6]. In addition to the deterministic propulsion, the trapped particle is also under the influence of Brownian motion, revealed as a blinking of the elastic scattering signal from the particle, as well as by the delimited fluctuations in λ_r (Fig. 1(b)). In what follows we will show that the physical interpretation of these fluctuations reveals the trapping potential and the size of the nanoparticle. This potential is responsible for increased transport of target nanoparticles to the sensing volume.

Fractional fluctuations in the resonance wavelength from the background level $\Delta\lambda_r/\lambda_r$ are clearly due to perturbations in the WGM as the result of nanoparticle's interaction with the microcavity, and are equal at each instant to the ratio of the energy polarizing the particle W_p to the energy in the cavity W_c (reactive sensing principle, RSP) [7],

$$\Delta\lambda_r/\lambda_r = W_p/W_c \tag{1}$$

#107949 - $15.00 USD Received 25 Feb 2009; revised 31 Mar 2009; accepted 31 Mar 2009; published 1 Apr 2009

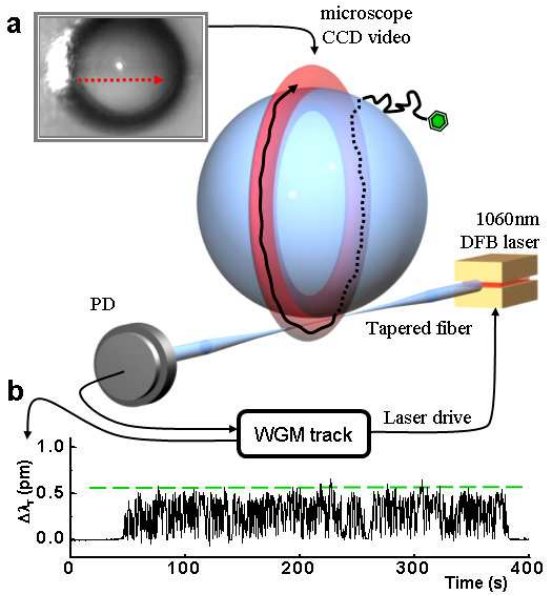

Fig. 1. WGM-Carousel-Trap. (a) WGM excited in a microsphere (radius R = 53 μm) with Q = 1.2×10^6 by a 1060nm tunable laser using fiber-evanescent-coupling. The resonance wavelength is tracked from a dip in the transmitted light (PD). An elastic scattering image shows a polystyrene particle (radius a = 375 nm) trapped and circumnavigating at 2.6 μm/s using a drive power of 32 μW. (b) A particle is sensed through resonance wavelength fluctuations $\Delta\lambda_r$ that identify its size/mass. These fluctuations are recorded from before the particle enters the Carousel-trap until after it escapes ≈ 6 min later.

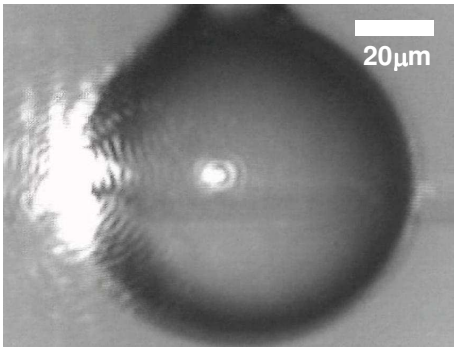

Fig. 2 (Media 1) This is a sped-up video (16× real time) of a single nanoparticle (a = 375 nm) being trapped and propelled by the WGM momentum flux. The fiber is coupled to the microsphere (R = 48 μm) by contact slightly off the equator on the backside. The WGM has Q = 1.5×10^6, and is driven with a power P = 25 μW. Light travels in the fiber from right to left (WGM scatter can be seen on the left edge of the microsphere). The trapped particle is observed through elastic scattering as a bright spot in front and in back of the microsphere. The ring pattern around the bright spot is caused by diffraction by the microscope objective. The nanoparticle is trapped, and propelled for just over two revolutions with a period of 140s before escaping. The particle appears to move faster on the backside due the transverse magnification in the microsphere image.

The shift $\Delta\lambda_r$ is therefore independent of the power driving the resonator but is proportional in a dipole approximation to the ratio of the intensity at the nanoparticle's center $\boldsymbol{r_c}$ to the energy in the mode; $\Delta\lambda_r(\boldsymbol{r_c}) \propto E_0^2(\boldsymbol{r_c}) \Big/ \left\langle \varepsilon(\boldsymbol{r}) E_0^2(\boldsymbol{r}) \right\rangle$, where E_0 is the electric field amplitude and $\varepsilon(\boldsymbol{r})$ is the modal permitivity. For the lowest order angular wave excited in our experiments the intensity function is symmetrical about the equator with a Gaussian-like shape, and falls

#107949 - $15.00 USD Received 25 Feb 2009; revised 31 Mar 2009; accepted 31 Mar 2009; published 1 Apr 2009

off at "latitudes" on either side with a characteristic width $w \approx 6$ μm. In contrast, in the radial direction the intensity falls off as the square of a spherical Hankel function which is well approximated by a decaying exponentially with a much shorter "evanescent length" $L \approx 150$ nm [8]. Images of the particle's orbit show it travelling along the equator with a root mean square transverse displacement to either side of < 1.5 μm. The time to diffuse over this distance for our typical nanoparticle is several seconds, whereas the observed fluctuations in $\Delta\lambda_r$ occur much faster: over a time scale associated with diffusion through a length ~ 100 nm. Consequently, these fluctuations are due to changes in the interfacial separation h between the nanoparticle's surface and the surface of the microsphere, with the maximum fluctuation occurring at $h \approx 0$ (i.e. green line in Fig. 1(b)). Translating other wavelength shift levels into h values is critical to our analysis. Fortunately, this translation is easily implemented. Based on the RSP [7] the wavelength shift for the nanoparticle's center at $h+a$ to that on the surface is

$$\frac{\Delta\lambda_r(h+a)}{\Delta\lambda_r(a)} = \frac{\exp[-(h+a)/L]}{\exp[-a/L]} = \exp[-h/L]. \qquad (2)$$

Equation (2) enables wavelength shift statistics to be transformed into separation statistics. The results are particularly revealing.

3. Trapping potential well

Figure 3(a) shows the separation histogram taken on a nanoparticle (a = 140 nm) that circumnavigated a microsphere for just over two orbits. A pronounced maximum is seen at $h \cong 35$ nm from the sensing surface. The peak is indicative of a surface repulsion that becomes more evident by translating these separation statistics into a potential curve using equilibrium statistical mechanics.

Under the assumption of thermal equilibrium the Boltzmann distribution relates the potential $U(h)$ to the probability density $p(h)$; $U(h) = -k_B T \ln[p(h)/p(h_{ref})]$, where h_{ref} is a reference separation for which $U(h_{ref}) = 0$. Figure 3(b) shows the result. The particle is clearly trapped in a radial potential well with its minimum 35 nm from the surface as it is driven to orbit by the WGM's tangential momentum flux. These potential points were fit by a sum of two exponentials: a short-range repulsive interaction $U_s / k_B T = 6.2\exp\left[-h/(17.6\text{ nm})\right]$, and a long-range attractive interaction $U_p / k_B T = -8.0\exp\left[-h/(142.7\text{ nm})\right]$. The latter supports our hypothesis that the particle's motion is principally radial since its characteristic length of 143 nm is close to the evanescent length in the radial direction (146 nm). The attractive force arising from this potential is similar to the gradient force in optical tweezer experiments, for which the potential in the equatorial plane is expected to be the negative of the polarization energy, $U_p(h) \approx -(\alpha_{ex}/4)E_0^2(a)\exp(-h/L)$ where α_{ex} is the nanoparticle's polarizability [9]. Indeed, a series of experiments show that the value of this "polarization potential" at the surface $U_p(0)$ is proportional to the power P entering the mode. The gradient force is aided in keeping the particle on an equatorial track by a transverse phase-gradient contribution [10]. The positive potential U_s is independent of power, and appears to be due to repulsion between ionized silanol groups on the bare silica surface (pH = 7), and the negatively charged polystyrene nanoparticle (the particles used were slightly sulfonated). The characteristic length of U_s is close to the Debye length λ_D arrived at from the measured conductivity of our medium [11], $\lambda_D \approx 20$ nm, assuming monovalent ions. By varying the ionic conductivity of the solution one can effectively change the range of U_s. In contrast, U_p is independent of ionic conductivity and reaches much deeper into the solution. In effect the combined potential forms a "sink-hole" that draws particles toward the optimal region in the sensing volume.

#107949 - $15.00 USD Received 25 Feb 2009; revised 31 Mar 2009; accepted 31 Mar 2009; published 1 Apr 2009

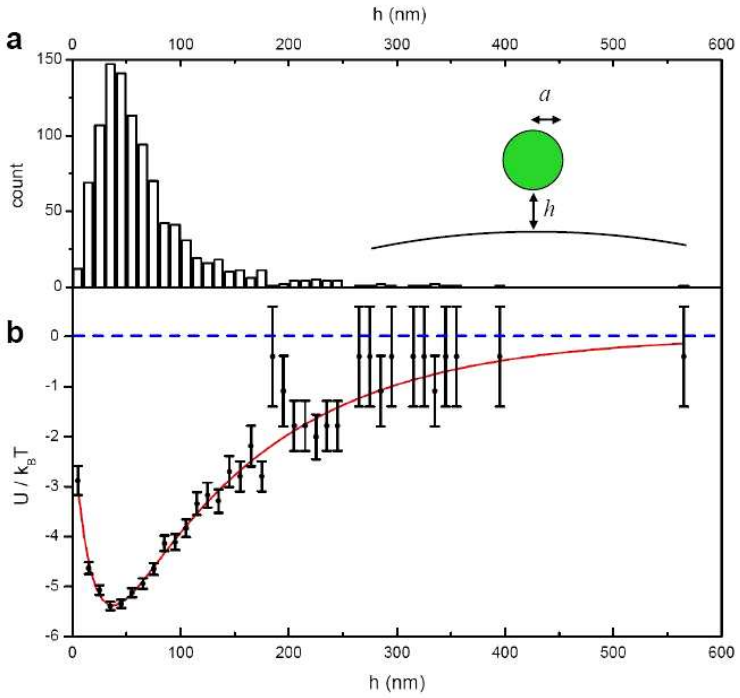

Fig. 3. Separation histogram and trapping potential. (a) separation histogram collected from a single tapping event of a polystyrene (PS) particle (from mean radius <*a*> =140 nm hydrosol). The WGM with $Q = 7.3\times10^5$ was excited with P = 233 μW at $\lambda \approx 1060$ nm in a microsphere with R = 44 μm. The statistics were comprised of 1000 points. (b) Potential plot arrived at from the histogram in (a). These points are fit to a sum of two potentials (in red).

It is important to point out that not all forces in the optical problem may be considered conservative. [10] Our description of a potential associated with the separation statistics is strictly meant to apply to conservative forces in the equatorial plane.

The value of the polarization potential at zero separation, $U_p(0)$, may be calculated directly in terms of the maximum wavelength shift $(\Delta\lambda_r)_{\max} = \Delta\lambda_r(a)$, the power P driving the mode, and its resonant Q by using the RSP, Eq. (1). [7] The polarization energy at zero separation $W_p(0) = - U_p(0)$ and the energy in the cavity W_c is the driving power P times the photon lifetime Q/ω_r. Consequently, the potential at zero separation is

$$U_p(0) = -\left(\Delta\lambda_r\right)_{\max} PQ / \left(2\pi c\right), \tag{3}$$

where c is the speed of light. Whereas $(\Delta\lambda_r)_{\max}$ is independent of P or Q, the attractive potential grows as their product. If we suppose U_s is very short range, then the minimum power to perceive trapping, $P_{\min}$, can be estimated by setting $\left|U_p(0)\right| \approx k_B T$;

$$P_{\min} \approx k_B T(2\pi c) / [Q\,(\Delta\lambda_r)_{\max}]. \tag{4}$$

Since all of the parameters on the right in Eq. (4) are measurable, the thermal escape hypothesis is testable by measuring $P_{\min}$.

A series of five experiments were performed in order to detect the minimum power to keep a particle in orbit. In each the power driving a WGM was lowered as an orbiting particle's velocity was measured from a video recording. Figure 4 shows the results of one of these experiments for which the power was lowered from 42 μW over a period of 1200 s. The particle was lost as the power reached 7.3 μW. At this power the normalized potential from Eq. (3) $\left|U_p(0)\right| \Big/ k_B T \approx 1$, consistent with thermal escape (as indicated by the top horizontal

#107949 - $15.00 USD Received 25 Feb 2009; revised 31 Mar 2009; accepted 31 Mar 2009; published 1 Apr 2009

scale in the Fig. 4). The recorded velocities in the Fig. 4 do not appear to be heading toward an intercept at the origin as might be expected. The reason lies in the fact that although the momentum flux at a given height decreases in proportion to drive power, the flux seen by the particle falls more rapidly, since the particle moves outward as the drive power decreases. The other four experiments showed similar results. The picture that evolves is of a particle attracted to the orbit and rapidly fluctuating radially above the equator by Brownian forces. This trapping mechanism also leads to enhanced detection rates in the WGM biosensor.

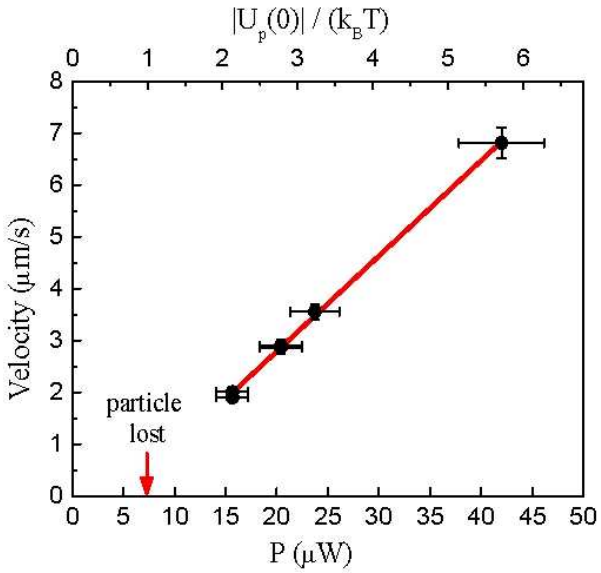

Fig. 4. Particle velocity as a function of drive power P. A nanoparticle of radius a = 375 nm was trapped in a Carousel of a microsphere with R = 45 μm and $Q = 1.5\times10^6$. The power was gradually reduced over a period of 1200 s. Upon reaching 7.3 μW the particle escapes within 10 s, as seen by imaging and through the cessation of wavelength fluctuations. The upper horizontal scale is calculated from Eq. (3).

Carousel trapping is expected to enhance binding rate detection in the following manner: The enhanced transport increases accumulation of particles in the sensing volume, and forced re-visitations by a particle to the surface increases the probability for finding a binding site. To measure the enhancement of the transport rates we compared the case of pure diffusion driven particles by operating at an arbitrarily low polarization potential $|U_p(0)|_d \approx 0.01\ k_BT$ to the case where the polarization potential was near the threshold for escape, $|U_p(0)|_e \approx 1k_BT$. These experiments were carried out for particles with a = 250 nm and for a concentration of 6 fM. In each case we counted the number of visitations to the sensing volume by registering the number of wavelength shift pulses exceeding $0.25(\Delta\lambda_r)_{max}$. For $|U_p(0)|_d$ we detected only one visitation to the sensing volume in 1 hour. However for $|U_p(0)|_e$, 49 visitations ~ 1 s in duration were detected in 1 hour. As the potential was increased to $|U_p(0)| > 5k_BT$, particles were strongly trapped in the Carousel, and accumulation of multiple particles over time became unavoidable. With $|U_p(0)|$ above $2k_BT$ trapping of a single particle for several minutes became highly probable, which allowed us to observe the delimited fluctuation. This limit, where the particle temporarily "touches" the surface, $(\Delta\lambda_r)_{max}$ provides a means for the determination of the particle size/mass.

The maximum wavelength shift signal $(\Delta\lambda_r)_{max}$ registered for a given laser-resonator combination appears to depend only on the size and dielectric properties of the orbiting nanoparticle. This signal occurs when the particle encounters the greatest evanescent field. As the drive power is raised more of these events occur, but the largest have the same limiting value. Theory was constructed early on that related this wavelength shift to the particle's polarizability and size by using the RSP [7, 12], but its confirmation has only come recently

#107949 - $15.00 USD Received 25 Feb 2009; revised 31 Mar 2009; accepted 31 Mar 2009; published 1 Apr 2009

with the observation and measurement of single wavelength shift steps in non-specific binding experiments [13]. However, these steps were random in size, associated with particles adsorbing at different latitudes on the sphere's surface where the sensing response can vary over orders of magnitude. In the Carousel mechanism, the particles are attracted to the equator, and therefore produce uniform response in the delimited fluctuation. This allows a nanoparticle to be sized without the need for binding. The RSP [7] provides an illuminating equation for describing the wavelength shift [13]

$$\left(\Delta\lambda_r\right)_{\max} \simeq D\,\frac{\lambda_r^{1/2}}{R^{5/2}}\,a^3\,e^{-a/L} \tag{5}$$

where D is a dimensionless dielectric factor equal to 2.26 for polystyrene in water. [8] Table 1 shows a comparison of particles sizes determined from $(\Delta\lambda_r)_{max}$, for separate experiments on single polystyrene nanoparticles caught in Carousel traps by inverting Eq. (5), with the mean size reported for a statistical number of particles by the manufacturer.

Table 1. Nanoparticle Sizing by WGM Carousel. Size determined for each of four Carousel trapped nanoparticles from their delimited wavelength shift $(\Delta\lambda_r)_{max}$ using Eq. (5) (far right) as compared with the mean size given by the manufacturer for the associated hydrosol <*a*>.

<*a*> (nm) $\sigma = 5\%$	λ (nm) Nominal	$R \pm 1.5$ (μm)	$(\Delta\lambda_r)_{max} \pm 0.02$ (pm)	*a* (nm) from RSP
140 ± 7	1059	43	0.25	158 ± 12
245 ± 12	1059	51	0.32	228 ± 19
245 ± 12	1312	56	0.42	247 ± 17
375 ± 19	1312	56	0.67	350 ± 21

Although the experiments were for resonators of different sizes and driven by different lasers, the nanoparticle size obtained by inverting Eq. (5) agreed with the manufacturer's mean size <*a*> within the uncertainties in the experiment and the standard deviation in the manufactured hydrosols. This clearly opens the door for a nanoparticle size/mass spectrometer in solution [14]. With a microsphere for which $R = 40$ μm and $Q \approx 10^7$ individual bioparticles having a mass of HIV (600 attograms, $a \approx 50$ nm) should be easily sizable with $P \approx 50$ μW at $\lambda \approx 780$ nm. For a power of 2 mW using the same resonator a smaller virus with $a = 15$ nm (mass ≈ 15 attograms, e.g. Poliovirus) is within reach.

Finally we return to the subject of binding. A particle caught in a Carousel orbit is in a pre-binding state which is easily converted to a binding state by reducing the range of the electrostatic repulsion and thereby allowing the optical force to pull a nanoparticle to the surface where the intrinsic van der Waal attraction can take hold. Decreasing the range of the electrostatic repulsion is accomplished by increasing the conductivity of the solution. Figure 5 shows two separate experiments on individual particles caught in Carousels for which the solution conductivities differed by an order of magnitude. The experiment at higher conductivity clearly shows the separation between the nanoparticle and the surface to be substantially reduced. An analysis of these separation statistics gave a repulsive potential for the low conductivity case corresponding to 0.5mM NaCl of $U_s / k_B T = 6.2\exp\left[-h/\left(17.6\text{ nm}\right)\right]$, whereas in the higher conductivity case corresponding to 5 mM NaCl $U_s / k_B T = 4.9\exp\left[-h/\left(6.1\text{ nm}\right)\right]$. The reduction in the range of the repulsive potential by a factor of 2.9 is close to the expected reduction in the Debye length. The later is known to be inversely proportional to the square root of the salt ionic strength, (reduction in range by 3.2). [11]

#107949 - $15.00 USD Received 25 Feb 2009; revised 31 Mar 2009; accepted 31 Mar 2009; published 1 Apr 2009

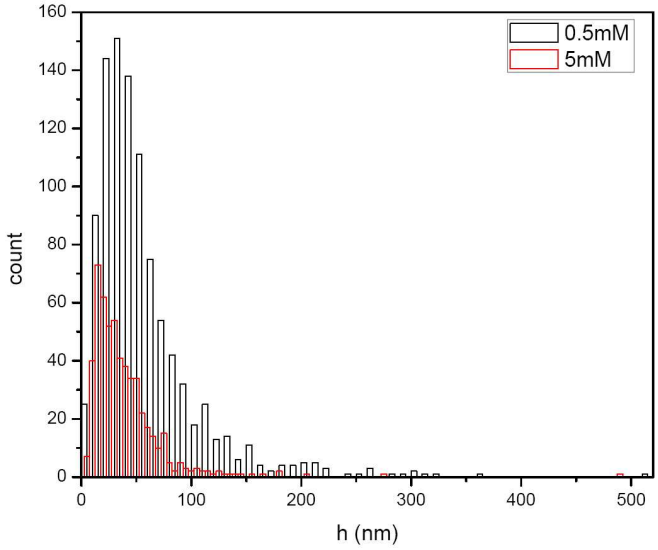

Fig. 5. Particle separation histograms for two different NaCl concentrations (0.5 mM and 5 mM). Note that the particle is closer to the surface for higher salt concentration, indicated by the peak position of the statistics.

By adding 20 mM of NaCl to our D_2O solution its conductivity was increased 40×. Nanoparticles (a = 375 nm) were trapped in the Carousel and bound to the surface. Figure 6(a) shows the first three binding events registered as uniform steps in $\Delta\lambda_r$. Although spatially random particle adsorption leads to a distribution of step heights which vary by more than an order of magnitude [13], the constancy of the step heights in Fig. 6(a) shows that the equator can be spatially isolated for binding. Such characteristics were also demonstrated with smaller nanoparticles (a = 140 nm). Figure 6(b) shows an experiment in which several of these particles bind to the Carousel surface from a 10 fM solution over a period of 20 minutes. In this case, there were two parallel paths, corresponding to a mode for which quantum number $m = l - 1$, indicating that the Carousel effect exists for higher order angular modes as well.

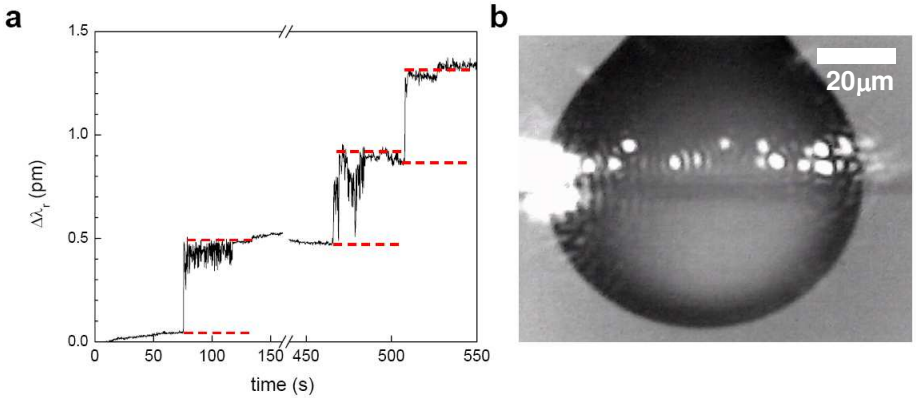

Fig. 6. (a) First three binding steps of nanoparticles (a = 375 nm) on a microsphere with R = 45 μm and P = 150 μW, Q = 2×10^5, Note the uniformity in step height. Red dash separation is set to 0.45 pm. (b) Image of a = 140 nm particles trapped and bound in the Carousel orbit, R = 39 μm.

4. Conclusions

In conclusion, the WGM Carousel mechanism provides underlying physics which answers the question posed in Ref. 4. We clearly see that detection rates are not limited by diffusion, and

#107949 - $15.00 USD Received 25 Feb 2009; revised 31 Mar 2009; accepted 31 Mar 2009; published 1 Apr 2009

can be increased by ~ 100×. In addition we discover that the new light-force mechanism provides a sensitive means for sizing individual particles and detecting their interactions with the sensor's surface. The effects produced by Carousel trapping should be difficult to avoid for viral sized nanopartices such as HIV or Influenza A, since the power needed to form the Carousel is < 200 μW. This power is orders of magnitude smaller than the trapping power reported with linear optical waveguides (~ 250 mW) [15]. Analytical and experimental studies show that our low trapping power is due to resonant build up within the spherical microcavity structure. In addition, by controlling the ionic strength and the trapping optical power, the particles are shown to bind preferentially within the Carousel. All of this provides optical WGM sensors with a distinct advantage not afforded to non-optical devices since the attractive potential reaches out into a solution and draws nanoparticles to the optimal sensing region unabated by ionic screening. In addition, proteins are also expected to interact with the Carousel, and light-force assisted functionalization of the resonator's equator is possible.

Acknowledgments

S. A. thanks D. G. Grier of NYU for useful discussions. This work was principally supported by the National Science Foundation - Division of Bioengineering and Environmental Systems Grant No: 0522668. D.K. thanks an NYU-POLY seed grant for partial support. F.V. was supported by a Rowland Junior Fellowship.

#107949 - $15.00 USD Received 25 Feb 2009; revised 31 Mar 2009; accepted 31 Mar 2009; published 1 Apr 2009